IAM LOSSES IN COLORED BIPV: FROM THE LAB TO THE FIELD

Anna Bertomeu i Baldé, Markus Babin, Nanna Lysgaard Andersen, Sune Thorsteinsson
Department of Electrical and Photonics Engineering, Technical University of Denmark
Frederiksborgvej 399, 4000 Roskilde, Denmark

ABSTRACT: The aesthetic challenge in deploying building-integrated photovoltaics (BIPV) is addressed by exploring coloration solutions, particularly absorptive materials. These, aside from the direct coloration losses, also introduce additional absorption and reflection losses, which increase with the incidence angle and vary significantly depending on the color. In this study, BIPV modules with colored interlayer foils are investigated, revealing significant differences in incidence angle modifier (IAM) behavior between the five colors studied. The Martin and Ruiz model captures the overall trend but faces difficulties in fitting the IAM of colored samples, especially when combined with satinated or structured glass. In contrast, the polynomial Sandia IAM model achieves a solid fit. Furthermore, this study compares the lab-determined angular optical losses with outdoor measurement data. This involves modeling effective irradiance and power output, accounting for color-dependent module efficiency, temperature effects, and IAM losses. The study also indicates that apart from IAM losses, spectral mismatch variation has a significant effect on the performance of colored BIPV.
Keywords: BIPV, IAM, colored BIPV, spectral variation

1 INTRODUCTION

The growing trend of integrating solar panels into buildings, known as BIPV, is a significant step towards decarbonizing the building stock. To ensure financial viability of these projects, accurately predicting the performance of these systems becomes fundamental. However, the electrical performance of BIPV can deviate from that of traditional PV systems due to their operation under different conditions, like higher operating temperatures, extreme tilts, non-optimal orientations, or the introduction of coloration for greater aesthetics [1].

To customize the appearance of BIPV systems to align with architectural demands, methods include the use of materials that exhibit spectrally selective absorption and reflection, positioned between the glass cover and the PV cell, as well as thin-film coatings.

This paper focuses on a specific aspect: the additional angular reflection losses introduced by absorptive materials in BIPV, which exhibit color-dependent variability. Previously, IAM losses have been estimated to amount to up to 5% extra loss due to the colorant itself [2]. The aforementioned study also identifies the refractive index as a key driving factor behind the fluctuations in IAM associated with color differences. However, IAM losses from colored BIPV have not, according to the authors' knowledge, been shown in the field before.

This study seeks to address this gap by comparing the angular losses of six mini modules measured in the lab with one of six modules placed outdoors, mounted in the curtain wall facing west of a small operational BIPV installation at DTU Risø Campus, using a similar bill of materials.

2 METHODOLOGY

2.1 Mini modules and modules preparation

Both sample types are manually fabricated using monocrystalline silicon solar cells with two busbars encapsulated in a glass-glass laminate. In the façade-mounted modules, the top glass is satinized through acid-etching, while IAM measurements in the lab are performed both on samples with satinated and standard PV glass.

The single-cell mini-modules have dimensions of 20x30 cm, while the full-sized modules contain 48 cells, leading to total module dimensions of 105.5x148.5 cm. Coloration is achieved through colored interlayers laminated between the cover glass and PV cells using additional layers of encapsulant. In total, five interlayer foils made from the same base material but with different colors were studied.

To determine the transmission losses caused by coloration, IV-curves at standard test conditions (STC) were measured on all samples.

2.2 Angular dependent reflection losses

The setup for indoors IAM measurements of the mini modules is the same as in [2] and consists of a rotatory platform with stepper motor where the samples are mounted and illuminated using collimated light from a laser-driven light source.

In the process of fitting the acquired experimental data, two models are employed and evaluated. The first model is based on the Martin and Ruiz formulation [3][4] represented by Eq. (1). The second model is a 5th-order polynomial function, as outlined by Sandia [5] and presented in Eq. (2).

$$IAM_{M\&R} = \frac{1 - \exp[-\cos(AOI)/a_r]}{1 - \exp(-1/a_r)} \quad (1)$$

$$IAM_{Sandia} = b_0 + b_1 AOI + \cdots + b_5 (AOI)^5 \quad (2)$$

The IAMs for the full-size modules are not directly measured, instead the parameter a_r and the coefficient vector b in Eq. (1) and Eq. (2), respectively, are extracted from measurements on the mini-modules with satinated glass were employed to model the performance of the larger modules.

2.3 Outdoors data acquisition and modeling

The studied set of 6 modules is integral to a curtain wall BIPV system located at DTU Risø campus (55.6958°N; 12.1052°E). This system takes the form of an office container featuring three PV arrays integrated into its east, south, and west facades. The focal point of this investigation lies with the west-facing façade, oriented at 275° azimuth, shown in Figure 1.

Each module is connected to a power optimizer, reporting the output power in 5-minute intervals, and outfitted with a back-of-module PT 100 temperature sensor. Irradiance on the façade is measured using an in-plane pyranometer, with irradiance components measured

10.4229/EUPVSEC2023/4BO.16.6
020289-001

at a nearby weather station (< 200 m). For more details on the system and data acquisition, refer to [6].

Figure 1: West-facing BIPV façade featuring five colored modules and one uncolored reference.

The main focus of this study is to explore the color-dependent IAM effect. To achieve this, the study involves creating a model for the DC power output of each module. This model is based on the module's efficiency as measured under Standard Test Condition (STC), temperature, and the in-plane irradiance. Additionally, the IAM effect is integrated into the irradiance model to understand how it impacts the overall performance of the modules. Subsequently, the predicted power output is compared to the measured performance in order to assess the model accuracy.

Equations (1) and (2) are applicable for introducing the IAM to the beam component of the plane-of-array irradiance. However, for increased accuracy, it is essential to extend the IAM effect to also encompass the diffuse and ground reflected components. This can be done by integrating over all angles contributing to the diffuse and reflected irradiance. Assuming isotropic distributions allows for use of an analytical approximation of these integrals based solely on PV module tilt β. Two variations of this approach which can be used to model the effective irradiance have been presented in literature:

The first approach by Martin and Ruiz [7], uses the angular loss coefficient a_r whereas in the second approach, equivalent Angles of Incidence (AOIs) for the diffuse and ground-reflected components are calculated based on work by Brandemuehl and Beckman [8]. Subsequently, these equivalent angles are used in the Sandia model in Eq. (2) to separately determine the irradiance components.

As input to this modelling, DNI and DHI are measured at the nearby weather station and used together with the Hay diffuse sky model for transposition and an albedo value of 0.22 to determine reflected irradiance. Furthermore, to facilitate steady-state temperature modeling, exclusively data originating from clear sky days is used.

2.4 External quantum efficiency

During the analysis phase, it was decided to also measure the external quantum efficiency (EQE) of the 6 mini modules. This is done to uncover potential explanations for observed discrepancies between the modeled and measured power output of the modules in the BIPV system under study.

PV Measurements' QEXL system with a 5 nm resolution is used to conduct the EQE measurements, based on calibration with a reference Si-photodiode for the wavelength range of 300-1100 nm. The IR range is calibrated separately using a Ge-photodiode.

2.5 Solar spectrum measurements

In order to estimate the effect of spectral variations on the differently colored modules during a clear-sky day (June 11, 2023), the EQE measurements described in section 2.4 are combined with measured DNI data. This data is acquired using an EKO MS711DNI spectroradiometer, mounted on a two-axis solar tracker at DTU Risø weather station, located approximately 200 m from the BIPV test installation. Spectral data is recorded in the range of 300 to 1100 nm at 5 minute intervals.

The mismatch factor (MM) is calculated according to Eq. (3), using the standard AM1.5 Direct spectrum as reference (G_{ref}). To allow for easier comparison between the different colors, their mismatch factor is put in relation to that of the uncolored reference according to Eq. (4).

$$MM = \frac{\int EQE \cdot DNI \, d\lambda}{\int EQE \cdot G_{ref} \, d\lambda} \cdot \frac{\int G_{ref} \, d\lambda}{\int DNI \, d\lambda} \quad (3)$$

$$MM_{rel} = \frac{MM(color)}{MM(reference)} \quad (4)$$

3 RESULTS AND DISCUSSION

3.1 Total optical losses

Figure 2 shows the measured short-circuit currents (I_{sc}) for all samples, relative to the uncolored reference. It shows coloration losses of approximately 20 to 40 % under STC conditions, depending on the color. While slight differences can be observed between façade-mounted modules and single-cell samples, both sets show similar trends for coloration losses depending on color.

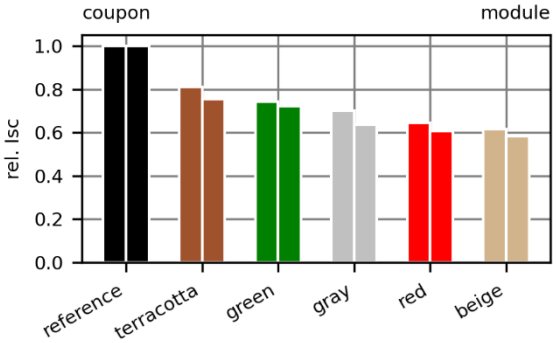

Figure 2: Relative short circuit current of coupon (left) and full-sized modules (right).

3.2 IAM losses

The IAM of the six mini modules with standard PV glass covers, obtained from the measurements in the lab, is presented in Figure 3, together with a fit of the Sandia IAM model. To isolate the effect of coloration from the angular dependent reflections from the glass cover, Figure 4 shows the IAM relative to the reference sample.

It can be observed that the difference in IAM with color is significant, however it is not directly correlated with the coloration loss shown in Figure 2. Comparable findings have also been documented for ceramic printing, demonstrating a lack of direct correlation between transmission losses and angular response. Instead, the increase

10.4229/EUPVSEC2023/4BO.16.6
020289-002

in optical losses with incidence angle is correlated with the refractive index of the coloration material, including pigments [2].

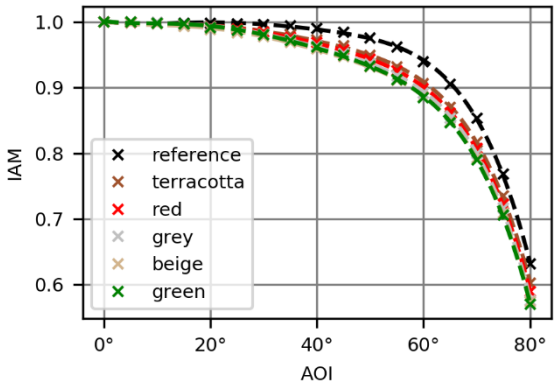

Figure 3: Measured (×) IAMs versus AOI, together with the Sandia fit (--), for each mini module with standard PV glass.

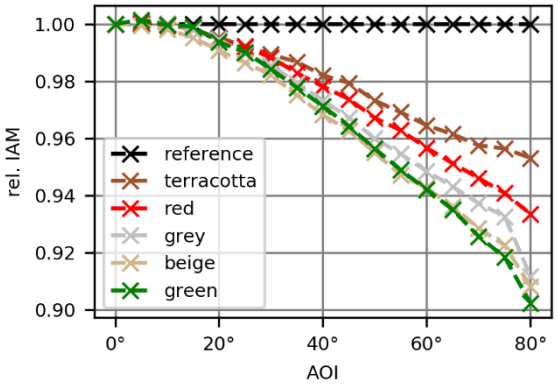

Figure 4: Relative IAM values versus angle of incidence, measured on mini modules with standard PV glass.

To investigate the fitting capabilities of IAM models, Figure 5 and Figure 6 show the measured and fitted IAM of the reference and terracotta-colored samples, with standard PV and satinated glass, respectively.

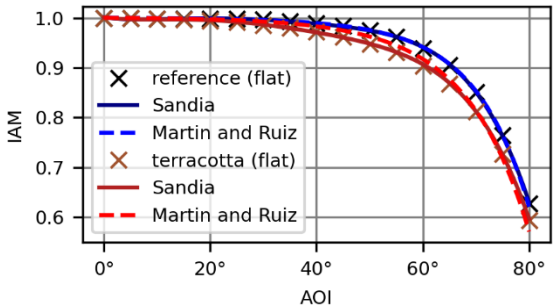

Figure 5: Measured (×) and fitted (-/--) IAM on reference and terracotta-colored samples with standard PV glass.

For samples with standard PV glass, the Martin and Ruiz model does capture the reduction in IAM with coloration, however, the model encounters difficulties in accurately fitting the measured data for incidence angles ranging from 30° to 60°. This error increases significantly when using satinated glass, as the Martin and Ruiz model is unable to capture the changed IAM profile accurately.

On the other hand, the Sandia model achieves a good fit for all samples, regardless of glass cover or coloration.

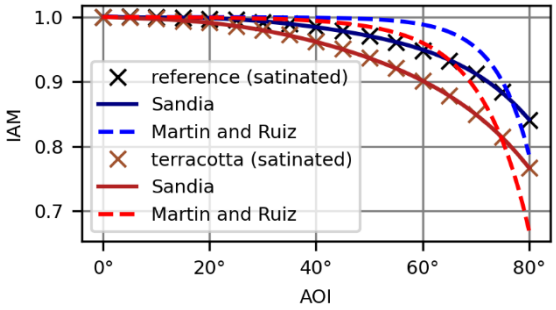

Figure 6: Measured (×) and fitted (-/--) IAM on reference and terracotta-colored samples with satinated glass.

3.3 Effect of IAM in the field

To identify the impact of including IAM models in outdoor performance modelling, Figure 7 shows the measured and modelled power of the terracotta-colored module over a clear-sky day. Solar noon on the shown day occurred at approximately 11:15 (UTC time) at the installation location.

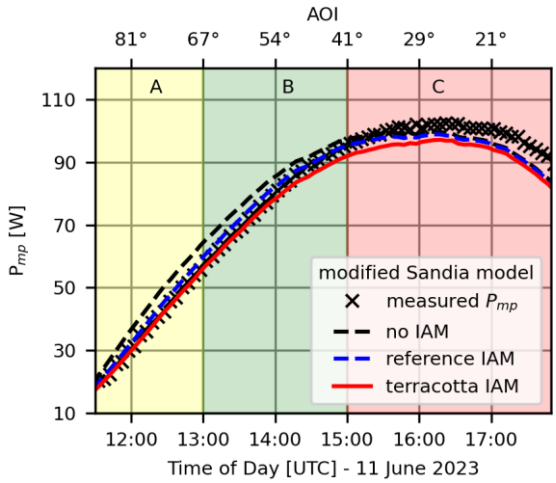

Figure 7: Comparison of P_{mp} values between measured (×) and modeled (-/--) data on a clear sky day for the terracotta-colored BIPV module.

When considering no IAM losses at all, module power output is significantly overestimated in the early afternoon (period A and B). By just considering the angular dependent reflections from the satinated glass surface using the Sandia fit of the reference sample, the fit of the measured data is significantly improved during the early and middle afternoon (period A and B). Considering the measured IAM of the terracotta sample further reduces the modelling error in these time periods, however a significant deviation remains between modelled and measured data in the later afternoon (period C). This discrepancy can be attributed to the fact that the solar spectrum undergoes variations throughout the day, as discussed in next section.

3.4 Intra-daily spectral variation effect

Figure 8 illustrates the impact of introducing a colored interlayer by comparing the external quantum efficiency of colored modules to the reference module. For all colors, the spectral response of the modules are shifted towards longer

10.4229/EUPVSEC2023/4BO.16.6
020289-003

wavelengths, albeit to different degrees.

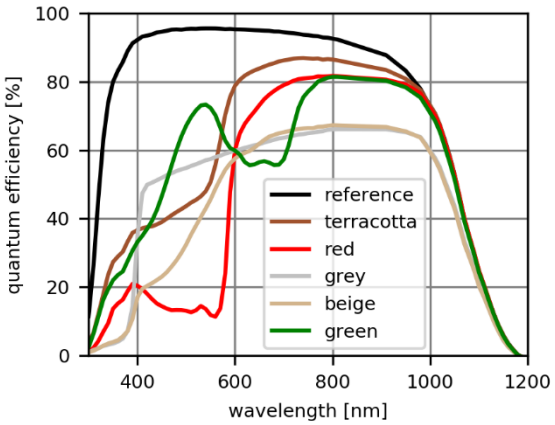

Figure 8: EQE laboratory measurements on the six mini modules.

Based on these measurements it can be hypothesized that such colored modules will perform better at times of day where the solar spectrum similarly shifts to higher wavelengths, i.e. the morning and evening. This is reinforced by the calculated relative mismatch factors shown in Figure 9: Here the red colored module experiences the highest increase in relative efficiency, as its spectral response shows the largest change. As shown by the air mass plotted on the secondary axis, this change in spectral mismatch gain is a direct function of light absorption and scattering in the atmosphere and therefore highly dependent on system location and orientation.

Since the model considered earlier did not account for the daily spectral variation, this provides an explanation for the underestimation of power for hours after 16:00 (UTC), as shown in Figure 7.

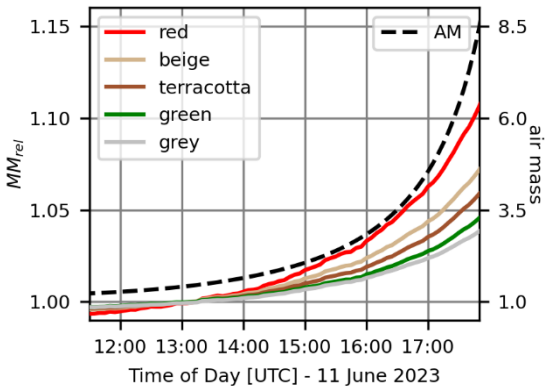

Figure 9: Calculated spectral mismatch for each module color relative to the uncolored reference based on spectral DNI and EQE, geometrical airmass on the right axis.

Implementing this spectral mismatch gain in the power modelling presented in section 3.3 results in Figure 10. It shows significant improvements in the late afternoon (period C). Despite improvements, some deviation remains, which could be associated with different spectral variations of diffuse and/or ground reflected light. Additionally, the isotropy-assumption for diffuse and reflected irradiance may be invalid during the late afternoon, due to the low solar elevation.

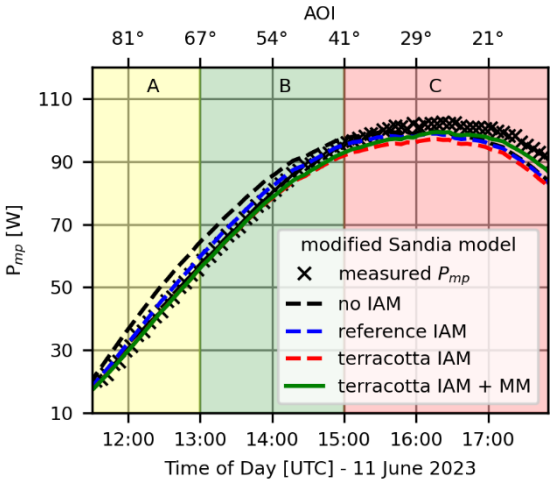

Figure 10: Comparison of P_{mp} values between measured (×) and modeled (-/--) data on a clear sky day for the terracotta-colored BIPV module.

For the specific orientation and location considered in the study, results suggest that it is important to consider daily spectral variation when modeling the effective irradiance, especially for colored modules with EQE curves that exhibit a primary response in the red range (around 600-1000 nm).

The above results are reported for a west facing façade at 56° latitude, where the AOI is at its minimum for high airmass. The airmass variation on a south facing façade is smaller and IAM impact might be larger. Similarly, different results with lower spectral mismatch factors and less daily variation are expected for diffuse lighting conditions.

4 CONCLUSIONS

As determined using indoor IAM measurements, the colored samples exhibit different angular responses compared to the reference sample, indicating distinct reflective properties for each color. While the Martin and Ruiz model effectively captures the general behavior for samples with standard PV glass, it encounteres challenges when fitting data for colored samples in the incidence angle range of 30° to 60°. Notably, it struggles to accurately model samples with satinated glass. On the other hand, the Sandia model provides a good fit based on a polynomial equation.

When bringing this to a colored BIPV installation in the field, it was found that the inclusion of added angular losses associated with glass surface structure, such as satination, as well as coloration-dependent IAM losses in modelling is critically important.

Further modelling errors were observed during the late afternoon on clear sky days. This discrepancy can in part be explained by the temporal evolution of the irradiance spectrum throughout the day. In the presented setup, since the colored modules are facing west, IAM losses are dominating in the early afternoon hours, whereas spectral mismatch losses are dominating in the later afternoon. In south-facing façade or rooftop installation, the strongest impact of these two effects may be seen at the same time, potentially leading to a significantly higher error in performance predictions. On the other hand, since both effects show opposite signs for red-colored modules, they

10.4229/EUPVSEC2023/4BO.16.6
020289-004

may partially compensate for each other.

While only a clear-sky day was investigated in this study, diffuse irradiation can be modeled using equivalent incidence angles greater than 55° [8]. Consequently, it can be expected that the IAM losses due to coloration increase in magnitude on overcast days.

In general, the results show that not accounting for color-dependent IAM losses and/or spectral mismatch can lead to significant errors for the daily energy yield on clear-sky days.

5 ACKNOWLEDGEMENTS

The authors acknowledge the support from EUDP as a funding agency for project “64021-1079 UnitSun”, and Rasmus Nielsen for or his assistance with the EQE experiments.

6 REFERENCES

[1] N. Martín-Chivelet, K. Kapsis, H. R. Wilson, V. Delisle, R. Yang, L. Olivieri, J. Polo, J. Eisenlohr, B. Roy, L. Maturi, G. Otnes, M. Dallapiccola, W.M. Pabasara Upalakshi Wijeratne. “Building-Integrated Photovoltaic (BIPV) products and systems: A review of energy-related behavior”. Energy and Buildings 262 (2022) 111998. https://doi.org/10.1016/j.enbuild.2022.111998

[2] M. Babin, S. Thorsteinsson, A. A. Santamaria Lancia, P. B. Poulsen, A. Thorseth, C. Dam-Hansen, M. L. Jakobsen. “Dependency of IAM Losses in Colored BIPV Products on the Refractive Index of Colorants”. Proceedings of 38th European Photovoltaic Solar Energy Conference (2022) pp. 583-589. https://doi.org/10.4229/EUPVSEC20212021-4BO.4.2

[3] N. Martin and J.M. Ruiz. “Calculation of the PV modules angular losses under field conditions by means of an analytical model”. Solar Energy Materials and Solar Cells 70 (2001) 25–38. https://doi.org/10.1016/S0927-0248(00)00408-6

[4] N. Martín and J. M. Ruiz. “A new model for PV modules angular losses under field conditions”. International Journal of Solar Energy 22 (2002) 19–31. https://doi.org/10.1080/01425910212852.

[5] D. L. King, E. E. Boyson, and J. A. Kratochvil. “Photovoltaic Array Performance Model”. Tech. rep. SAND2004-3535. Sandia National Laboratories, 2004.

[6] A. Bertomeu i Baldé. “Performance model validation of BIPV curtain walls”. Master Thesis. DTU Department of Electrical and Photonics Engineering (2023). https://findit.dtu.dk/en/catalog/64c6fbec5334821f4f64121c

[7] N. Martín and J. M. Ruiz. “Annual angular reflection losses in PV modules”. Progress in Photovoltaics: Research and Applications 13 (2005) 75–84. https://doi.org/10.1002/pip.585

[8] M. Brandemuehl and W. Beckman. "Transmission of diffuse radiation through CPC and flat plate collector glazings". Sol. Energy 24 (1980) 511–513. https://doi:10.1016/0038-092X(80)90320-5